Diffusion from Spheres in a Continuous-Flow Stirred Tank

Solvent diffusion from spheres at constant mass-transfer Fourier number, Fo_M, in a single continuous-flow stirred tank (CFST) and in a series of CFSTs is simulated. A transfer efficiency is defined and transfer efficiency curves are constructed as a function of Fo_M and the residence time distribution of the spheres in the system. The fraction of solvent removed from the spheres in a series of CFSTs can be approximated using the transfer efficiency curves and knowledge of the operating conditions in each tank. The usefulness of the curves to predict solvent removal from polymer spheres under pilot-plant conditions is examined.

Kevin J. Liekhus
Thomas R. Hanley
Department of Chemical Engineering
FAMU/FSU College of Engineering
Tallahassee, FL 32316

Introduction

Solvents are used in polymer processes to change the physical state of the polymer to facilitate transfer through the process; to aid in the fabrication of polymer spheres, films, and other end products; and to serve as a medium in solution polymerization reactions. After serving its purpose, the continued presence of the solvent in the polymer is usually not desirable. The solvent needs to be removed to regain desirable physical properties of the polymer, to recoup and recycle valuable solvent, or to reduce solvent emissions into the environment. The manufacture of polymeric spheres is an area of growing commercial importance. Spheres provide a high area-to-volume ratio and an optimum shape for mass transfer (adsorption, desorption) and energy transfer (combustion, conduction) where high surface area and a uniform shape are desirable. Polymeric spheres are used in separation processes and a potential need exists for spheres of new species-specific polymer resins useful in biochemical separations. The production of polystyrene microspheres for chromatography column packing (Chiang and Prudhomme, 1988) and polyoxyphenylene microspheres (Abe et al., 1987) has been described in the literature. Nitrocellulose lacquers (Durrans, 1971) form the foundation for gunpowder. Depending on the polymer–solvent system, the solvent is removed from the spheres in a gaseous or liquid medium in a batch or continuous-flow process.

The description of unsteady-state diffusion in a single sphere of constant radius for a variety of initial, boundary, and operating conditions has been reviewed by Crank (1956). Sphere systems with various initial concentration profiles and constant or time-varying surface concentration were also examined. Solvent removal from spheres in a batch or semibatch system is more likely to yield a uniform final product. A continuous-flow system offers the advantages of reduced labor and operating costs but with the increased likelihood of a distribution of exiting spheres with differing solvent content. The study of diffusion from spheres in continuous-flow stirred tanks has not received much attention due, in part, to the small number of such commercial processes. Many diffusion processes are performed in batch because of the inherent problems of continuous-flow systems. The growing commercial importance of polymer processes, which may require solvent removal from spherical particles resulting from design or circumstance, suggests that a comprehensive examination of such continuous-flow systems is timely.

In this work, the diffusion of a solvent from spheres at constant mass-transfer Fourier number, Fo_M, in a continuous-flow stirred tank (CFST) and in a series of CFSTs is simulated. A transfer efficiency is defined and transfer efficiency curves are constructed as a function of Fo_M and the agitation conditions in the system. The fraction of solvent removed from the spheres in the series of vessels can be approximated using the transfer efficiency curves and knowledge of the operating conditions in each tank. In addition, solvent removal from shrinking polymer spheres in a continuous-flow stirred evaporator is investigated and the application of the efficiency curves to predict the solvent removal from polymer spheres is examined.

Diffusion from Spheres in One CFST

A CFST with an entering stream of spheres of uniform and constant size with an initially uniform concentration profile and constant solvent diffusivity is considered. The fraction of solvent

removed from a sphere in a CFST for time θ is

$$f(\theta) = 1 - \int_0^1 C(\theta, r) r^2 \, dr = 1 - C(\theta)_m \qquad (1)$$

where $C(\theta)_m$ is the mean concentration at time θ, and the concentration $C(\theta, \bar{r})$ in the sphere is defined by the transport equation

$$\partial C/\partial\theta = Fo_M[\partial^2 C/\partial r^2 + (2/r)\partial C/\partial r] \qquad (2)$$

with arbitrary boundary conditions. The fraction of solvent removed from all the spheres in a CFST is

$$\phi = \int_0^\infty f(\theta) E(\theta) \, d\theta = 1 - C_m \qquad (3)$$

where C_m is the overall mean concentration in the exiting spheres. The quantity $E(\theta)\, d\theta$ is the probability that spheres had a residence time in the CFST between θ and $\theta + d\theta$. The tanks-in-series model (Levenspiel, 1972) will be used to define the residence time frequency distribution, $E(\theta)$. The model parameter, N, is an integer varied to describe mixing conditions in the system. The fraction of solvent removed from spheres of uniform concentration entering an ideal CFST ($N = 1$) as a function of equilibrium solvent concentration at the surface is shown in Figure 1. The fraction of solvent removed from all the spheres, ϕ, is proportional to the quantity $(1 - C_\infty)$. This proportionality constant is defined as a transfer efficiency, ξ,

$$\xi = \phi/(1 - C_\infty) \qquad (4)$$

In this case, ξ is only a function of Fo_M and is independent of C_∞.

For the case when the boundary condition at the sphere surface is defined by a convective environment

$$\partial C/\partial r = Sh[C(\theta, 1) - C_\infty] \qquad (5)$$

the effect of the Sherwood number, Sh, and Fo_M on ξ in an ideal CFST is shown in a series of curves in Figure 2. The transfer efficiency increases with Sh until further increases ($Sh \geq 10^4$) do not alter ξ. For the cases where $Sh \geq 10^4$, the boundary condition

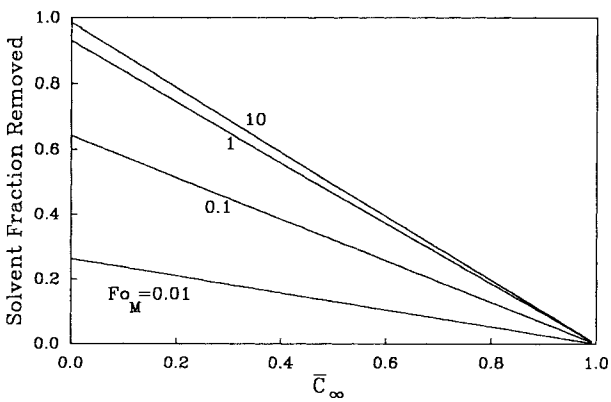

Figure 1. Fraction of all solvent removed from uniform, constant-size spheres.
Initially uniform solvent concentration profile, constant surface concentration (C_∞), in an ideal CFST

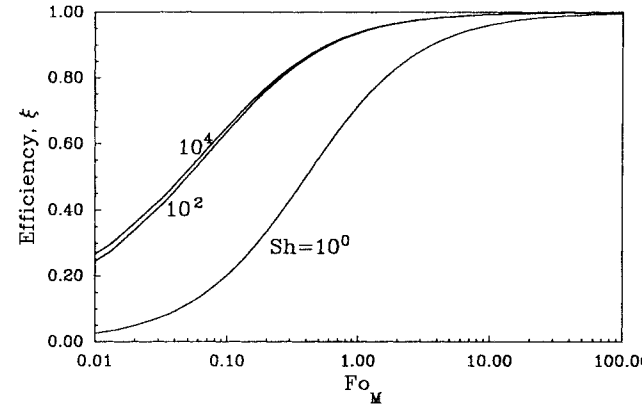

Figure 2. Effect of convective environment on transfer efficiency from uniform, constant-size spheres.
Initially uniform solvent concentration profile in an ideal CFST

is effectively equivalent to assuming a constant surface concentration. In such systems, ξ can be determined independent of specific knowledge of the ambient conditions.

The effect of the sphere residence time distribution (RTD) on ξ in a high Sh environment is shown in Figure 3. For low and intermediate values of Fo_M, the sphere RTD must be considered when specifying operating conditions. More specifically for the condition of constant Fo_M, as the standard deviation of the sphere RTD decreases (N increases), ξ increases. As N approaches infinity, the sphere RTD describes plug flow. The more practical significance for the case of $N = \infty$ is that it is equivalent to the design assumption that all the spheres experience the same mean residence time in the CFST. The transfer efficiency predicted using a mean particle residence time ($N = \infty$) is always greater than when the complete sphere RTD is used to determine ξ. The difference is greatest for all RTD at $Fo_M = 0.25$. The difference is negligible at high values of Fo_M.

Diffusion from Spheres in a Series of CFST

The equations used to determine the solvent fraction removed in a single CFST can be extended to a series of CFSTs. The

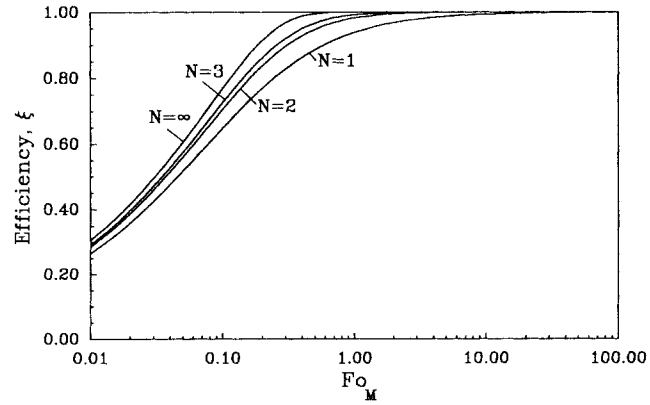

Figure 3. Effect of sphere residence time distribution (tank-in-series model) on transfer efficiency from uniform, constant-size spheres.
Initially uniform solvent concentration profile in an ideal CFST ($Sh = 10^4$)

fraction of solvent removed from a sphere in a second tank that left the first tank at θ_i, after residing θ_j in the second tank is

$$f(\theta_j, \theta_i) = \left[C_{m,i} - \int_0^1 C(\theta, r) r^2 dr\right] \Big/ C_{m,i} \qquad (6)$$

where $C_{m,i}$ is the mean solvent concentration in the spheres exiting the first CFST at time θ_i. The fraction of solvent removed in the second CFST from spheres that exit the first CFST at θ_i is

$$\phi(\theta_i) = \int_0^\infty f(\theta_j, \theta_i) E(\theta_j)\, d\theta_j \simeq \sum_{j=1}^{M_2} f(\theta_j, \theta_i) E(\theta_j) \Delta\theta_j \qquad (7)$$

The fraction of solvent removed from all spheres in the second CFST is

$$\phi_2 = \int_0^\infty \phi(\theta_i) E(\theta_i)\, d\theta_i \simeq \sum_{i=1}^{M_1} \phi(\theta_i) E(\theta_i) \Delta\theta_i \qquad (8)$$

The total solvent fraction removed from all spheres after passing through two CFSTs, ϕ_2^*, is defined in terms of ϕ_1 and ϕ_2 as

$$1 - \phi_2^* = (1 - \phi_1)(1 - \phi_2) \qquad (9)$$

If the number of time intervals in Eqs. 7 and 8 are $M_1 = M_2 = M$, the number of calculations required to determine the fraction of solvent in two CFSTs will be proportional to M^2. The computational time required to model solvent diffusion in two or more CFSTs in series will be extensive for large values of M. A quick method to approximate the fraction of solvent removed in a series of CFSTs is described below.

If the spheres of uniform size with a uniform concentration profile are assumed to enter each of a series of vessels, the overall fraction of solvent removed after I tanks, ϕ_I^*, is defined as

$$1 - \phi_I^* = \prod_{i=1}^{I} \{1 - \xi_i + \xi_i [C_{\infty,i}/(1 - \phi_{I-1}^*)]\} \qquad (10)$$

where $C_{\infty,i}$ is the dimensionless equilibrium concentration in the ith vessel. Thus, knowing the operating and agitation conditions in each CFST and using the transfer efficiency curves, the overall fraction of solvent removed from spheres in a series of CFSTs can be estimated.

A comparison of ϕ_I^* determined from Eqs. 9 and 10 for spheres passing through two CFSTs in series under a number of different operating conditions is summarized in Table 1. An implicit finite-difference method was used to solve Eq. 2. The results of the numerical method were compared to the analytical solution for diffusion from a sphere with a constant surface concentration by Crank (1956). The error in ξ was less than 0.1%. Each vessel was assumed to be perfectly mixed and $Sh = 10^4$. The transfer efficiency is determined as a function of Fo_M in each CFST from Figure 3.

Since the assumptions describing the entering spheres in a single CFST are the same, the two equations predict the same ξ_1 and ϕ_1^*. However, Eq. 10 assumes that all spheres entering the second CFST have the same uniform concentration profile, while Eq. 9 follows the spheres from the first CFST to the second. Values of ϕ_I^* calculated from Eq. 10 are always greater than values from Eq. 9. Equation 9 calculates the "correct" value of ϕ_2^* and is limited in accuracy only by the number and size of the time intervals used. As ϕ_2^* approaches the equilibrium value defined by the ambient environment, the difference between the two equations becomes negligible. This condition is met under most circumstances except when ξ is low (<0.75) in both CFSTs. Most practical designs would normally not operate at conditions that would yield low transfer efficiencies in all vessels.

Solvent Diffusion from Polymeric Spheres

The use of the transfer efficiency curves to predict solvent removal from polymeric spheres in a series of continuous-flow stirred evaporators (CFSE) is examined. Pilot-plant experiments to remove ethyl acetate from nitrocellulose spheres in a series of CFSEs were performed over a range of operating conditions. The spheres contain a small fraction of water, which affects the transport properties in the polymer. The polymer and solvent are blended together, extruded, and shaped into spheres in processes upstream from the evaporators. The free liquid phase in the evaporator consists primarily of water and solvent. The pilot-plant tests were conducted in CFSEs of approximately 0.34 and 0.11 m^3 in series. After a period of approximately four residence times, samples of the inlet and outlet streams from both evaporators were collected to determine the solvent composition in each phase. An experimental transfer efficiency can be defined for each trial as

$$\xi = \frac{\begin{array}{c}\text{solvent mass in sphere}\\ \text{entering vessel}\end{array} - \begin{array}{c}\text{solvent mass in sphere}\\ \text{exiting vessel}\end{array}}{\begin{array}{c}\text{solvent mass in sphere}\\ \text{entering vessel}\end{array} - \begin{array}{c}\text{solvent mass in sphere}\\ \text{residing until } t \to \infty\end{array}} \qquad (11)$$

Equation 11 requires the composition and mass of the spheres entering and exiting each evaporator and at equilibrium conditions. In a polymer–solvent system above the glass transition temperature, sphere shrinkage will occur with solvent removal (Chiang and Prudhomme, 1988). The overall sphere density is

Table 1. Overall Fraction of Solvent Removed from Spheres in Two Ideal CFSTs in Series ($Sh = 10^4$)

Case	$Fo_{M,1}$	$C_{\infty,1}$	ξ_1	ϕ_1^*	$Fo_{M,2}$	$C_{\infty,2}$	ξ_2	ϕ_2^* Eq. 9	ϕ_2^* Eq. 10
1	0.01	0.01	0.2648	0.2621	0.01	0.01	0.2648	0.3797	0.4548
2	0.10	0.01	0.6473	0.6408	0.10	0.01	0.6473	0.8270	0.8668
3	0.05	0.05	0.5152	0.4894	10.0	0.05	0.9926	0.9456	0.9466
4	1.00	0.05	0.9377	0.8908	1.00	0.01	0.9377	0.9823	0.9838
5	1.00	0.02	0.9377	0.9190	10.0	0.01	0.9926	0.9893	0.9895

defined assuming additive volumes of each component

$$\rho = (w_s/\rho_s + w_h/\rho_h + w_p/\rho_p)^{-1} \tag{12}$$

The initial polymer mass in the sphere remains constant during the solvent removal process, therefore, the transfer efficiency can be defined from experimental data as

$$\xi = \frac{w_{so} - w_{se}(w_{po}/w_{pe})}{w_{so} - w_{s\infty}(w_{po}/w_{p\infty})} \tag{13}$$

where the polymer weight fraction, w_p, is defined in terms of the measured weight fractions of solvent s and water h in the sphere. The solvent equilibrium mass fraction in the sphere was defined from an empirical equation as a function of the solvent mass fraction in the liquid. A semibatch evaporator was maintained at a constant temperature over a range of 70–100°C. After the spheres remained in the vessel for 3 h, the solvent compositions in the liquid and polymer were determined. The empirical relationship developed was

$$w_{s\infty} = 0.0485 + 5.85x_{s\infty} \tag{14}$$

Since the polymer density does not remain constant it is more convenient to express ξ and the polymer–liquid equilibrium in terms of mass fractions, which are required to define the density and solvent diffusivity. The experimental range of $x_{s\infty}$ was from 0.0015 to 0.021. The correlation coefficient of Eq. 14 was 0.996.

Vrentas and Duda (1979a) used the free-volume theory of transport to define solvent diffusivity as a function of temperature and concentration in concentrated polymer–solvent solutions. Vrentas and Duda (1977, 1979b) and Vrentas et al. (1984) developed the equations to describe concentration and temperature dependence of the solvent diffusion coefficient in a polymer–solvent–solvent system

$$D_s = \overline{D}_{0s} \exp(-E/RT) \cdot \exp\left[\frac{(w_s V_s^* + w_h V_h^* \chi_{sp}/\chi_{hp} + w_p V_p^* \chi_{sp})}{w_s(f/\gamma)_s V_s^o + w_h(f/\gamma)_h V_h^o + w_p(f/\gamma)_p V_p^o}\right] \tag{15}$$

The parameters for the diffusion coefficient of the nitrocellulose–ethyl acetate–water system were estimated from knowledge of data for the pure components and two-component systems. The parameters used to estimate the diffusivity of ethyl acetate in a nitrocellulose–ethyl acetate–water system during the pilot-plant trials are summarized in Table 2. The approximate sphere size and composition are known at the beginning of the entire process. The sphere size entering the first evaporator can be derived from knowledge of the sphere composition determined just before the evaporator, a polymer material balance, and Eq. 12.

Table 2. Estimated Parameters Used to Define Solvent Diffusivity in Pilot-Plant Trials

$V_s^* = 0.867$	$(f/\gamma)_s V_s^o = 0.139$
$V_h^* \chi_{sp}/\chi_{hp} = 3.5$	$(f/\gamma)_h V_h^o = 0.167$
$V_p^* \chi_{sp} = 0.48$	$(f/\gamma)_p V_p^o = 0.018$
$-E/RT = 47.9 - 1{,}866T/(T - 226.2)^2$	$D_{0s} = 0.00219$ cm^2/s

Results

The experimental ξ are plotted as a function of the initial Fo_M. The initial Fo_M consists of a solvent diffusivity and sphere radius defined in terms of the average composition in the sphere entering the evvporator. In addition, the solvent diffusivity is defined at the temperature in the CFSE. Experimental ξ are compared to the constant Fo_M efficiency curves over a variety of operating conditions. The experiments covered a range of Fo_M from 10^{-3} to 10^4. Experimental ξ at low to moderate values of Fo_M are shown in Figures 4–6 and at high values of Fo_M in Figures 7 and 8. Horizontal lines defined by the initial and final Fo_M show the decrease of Fo_M during the trial. Some of the lines for trials with high initial Fo_M are omitted for clarity. In these cases, the final Fo_M is near unity. Error bars are assigned to each calculated ξ resulting from the inherent limitations in determining each term in Eq. 12. The error was determined assuming $\Delta w_{so} = 0.005$, $\Delta w_{se} = 0.005$, $\Delta w_h = 0.005$, and $\Delta w_{s\infty} = 0.003$.

At high Fo_M (>10), the spheres reached equilibrium conditions ($\xi = 1$). In the region of moderate Fo_M ($0.1 < Fo_M < 10$), the experimental ξ are less than the corresponding values on the transfer efficiency curves. At low Fo_M (<0.1) the data are much more scattered about the curves. The solvent content in the spheres entering the second evaporator is much less (0.15–0.25 solvent mass fraction) than for those spheres entering the first evaporator (0.50–0.70 solvent mass fraction). In addition, the total solvent loss is less in the second evaporator. As a result, the experimental ξ at low Fo_M have larger relative experimental errors.

In all trials, the exit value of Fo_M is one to two orders of magnitude lower than the initial Fo_M. The variable Fo_M does not present a problem at high initial Fo_M since ξ is at or near unity over the entire range of Fo_M. However, at low initial Fo_M, ξ can decrease significantly over the range. This presents a problem in predicting ξ in spheres at low initial Fo_M. An increase in the mean sphere residence time or operating temperature can increase the initial Fo_M to ensure a high transfer efficiency. In those situations when Fo_M cannot be adjusted, it is important to be able to accurately estimate ξ at low Fo_M. If the experimental ξ are plotted against the range of Fo_M observed in the CFSE, the resulting line usually intersects the transfer efficiency curves at values of Fo_M less than the initial value. It would be more

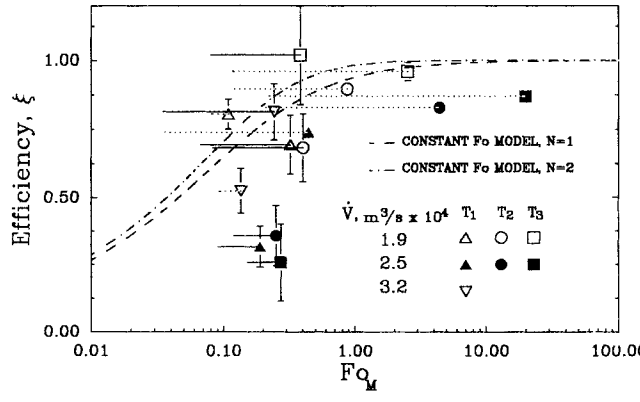

Figure 4. Transfer efficiency and change in FO_M for spheres (R_o = 0.058 cm) in two CFSEs in series.
Temp. in first/second evaporator: T_1 = 74°/77°; T_2 = 76°/79°; T_3 = 78°/81°
···· first evaporator; ——— second evaporator

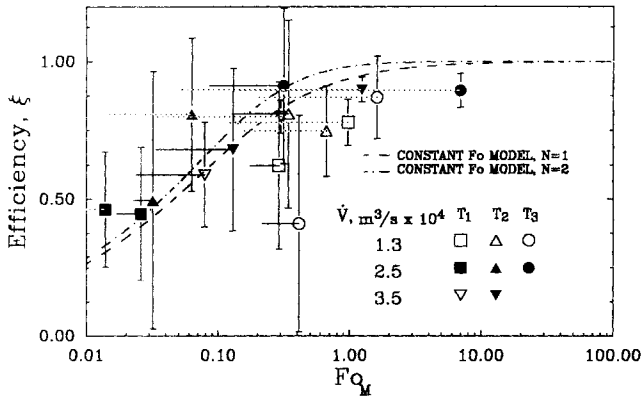

Figure 5. Transfer efficiency and change in Fo_M for spheres (R_o = 0.090 cm) in two CFSEs in series.
Temp. and symbols as in Figure 4

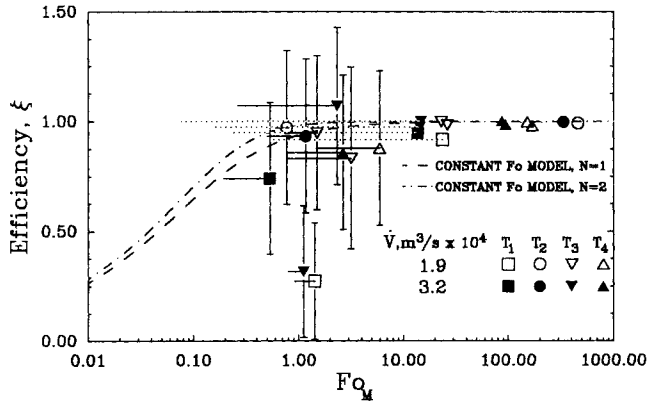

Figure 7. Transfer efficiency and change in Fo_M for spheres (R_o = 0.058 cm) in two CFSEs in series.
Temp. in first/second evaporator: T_1 = 75°/81°; T_2 = 78°/84°
· · · · first evaporator; —— second evaporator

appropriate that a characteristic Fourier number, Fo_M^*, be defined to represent the conditions observed by the spheres in the vessel.

The primary reason for the reduction of Fo_M is the decrease of the solvent diffusivity with decreasing solvent content in the sphere. As noted earlier, the reduction can be up to two orders of magnitude. The sphere size also changes upon solvent removal. Therefore, a characteristic $(D/R^2)^*$ is proposed

$$\left(\frac{D}{R^2}\right)^* = \int_{w_{so}}^{w_{se}} \frac{[D(w_s)/R^2(w_s)]\,dw_s}{(w_{se} - w_{so})} \tag{16}$$

The effect of changing sphere radius on Fo_M^* is less dramatic and can be accounted for by a mean solvent mass fraction, w_{sm}, thus simplifying Eq. 16

$$\left(\frac{D}{R^2}\right)^* = \frac{1}{R^2(w_{sm})} \int_{w_{so}}^{w_{se}} \frac{D(w_s)dw_s}{(w_{se} - w_{so})} \tag{17}$$

where $w_{sm} = (w_{se} + w_{so})/2$. An algorithm to define Fo_M^* in order to better estimate ξ for design purposes is outlined below:

1. Identify sphere composition and size entering CFST, mean sphere residence time, and equilibrium condition in CFST.
2. Calculate initial Fo_M.
3. Identify ξ at Fo_M from transfer efficiency curves in Figures 2 and 3.
4. Calculate ϕ^* and final sphere composition and size.
5. Calculate $(D/R^2)^*$ and $Fo_M^* = \tau(D/R^2)^*$.
6. Repeat steps 3 and 4 based on Fo_M^*.

Example

Equations 16–17 and the design algorithm are used to estimate the ξ and ϕ for spheres in two CFSTs in series. Values chosen to represent operating conditions in the CFST are similar to those seen in the pilot-plant trials. It is assumed that the mass of the polymer and water in the sphere remain constant while solvent diffuses out. The low water content and the decreasing water diffusivity in the polymer with decreasing solvent content are two reasons why this is observed in the pilot-plant trials.

1. R_o = 0.136 cm; w_{so} = 0.68; w_{ho} = 0.03; T_1 = 78°C; τ_1 = 22 min; $x_{s\infty,1}$ = 0.0185
2. Using Eq. 15, initial $Fo_{M,1}$ = 7.1

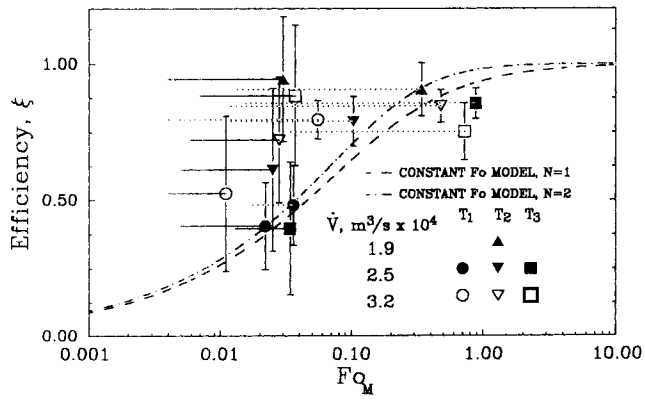

Figure 6. Transfer efficiency and change in Fo_M for spheres (R_o = 0.136 cm) in two CFSEs in series.
Temp. and symbols as in Figure 4

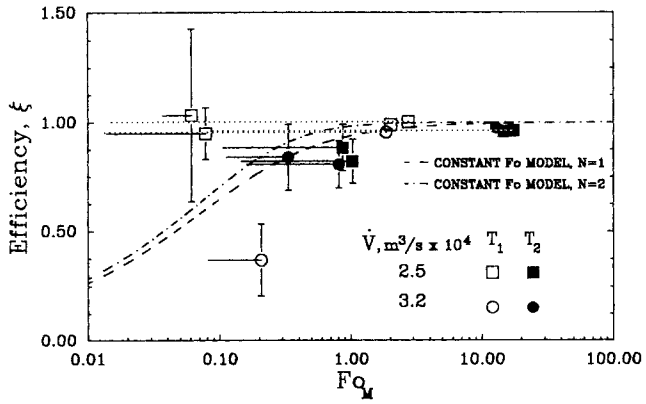

Figure 8. Transfer efficiency and change in Fo_M for spheres (R_o = 0.136 cm) in two CFSEs in series.
Temp. in first/second evaporator: T_1 = 75°/81°; T_2 = 78°/84°
· · · · first evaporator; —— second evaporator

3. $\xi_1 = 1.0$

4. Using a form of Eq. 10,

$$1 - \phi_1^* = 1 - \xi_1 + \xi_1(w_s\rho V)_{\infty,1}/(w_s\rho V)_o; \quad \phi_1^* = 0.912;$$

$$w_{s1} = 0.157; \quad w_{h1} = 0.079; \quad R_1 = 0.090 \text{ cm}$$

5. Using Eqs. 15 and 17, and the assumptions of constant water and polymer mass in sphere,

$$(D/R^2)_1^* = 1.7 \times 10^{-3}\,\text{s}^{-1}; \quad Fo_{M,1}^* = 2.3$$

6. $\xi_1 = 0.97$; $\phi_1^* = 0.886$; $w_{s1} = 0.195$; $w_{h1} = 0.075$; $R_1 = 0.092$ cm

7. In the second evaporator: $T_2 = 84°\text{C}$; $\tau_2 = 7.5$ min; $x_{s\infty,2} = 0.015$

8. Initial $Fo_{M,2} = 0.14$

9. $\xi_2 = 0.71$

10. $1 - \phi_2^* = (1 - \phi_1^*)\{1 - \xi_2 + \xi_2[(w_s\rho V)_{\infty,2}/(w_s\rho V)_o]/(1 - \phi_1^*)\}$; $\phi_2^* = 0.914$ $w_{s2} = 0.154$; $w_{h2} = 0.079$; $R_2 = 0.090$ cm

11. $(D/R^2)_2^* = 1.5 \times 10^{-4}\,\text{s}^{-1}$; $Fo_{M,2}^* = 0.067$

12. $\xi_2 = 0.57$; $\phi_2^* = 0.909$; $w_{s2} = 0.162$; $w_{h2} = 0.079$; $R_2 = 0.090$ cm

Conclusions

In general, the transfer efficiency curves can be used to specify optimum operating conditions to ensure high transfer efficiency. The proper design of a CFST for solvent removal from polymer spheres requires accurate knowledge of the solvent diffusivity in the polymer as a function of the solvent mass fraction and temperature; of the average composition entering the CFST; and of equilibrium data defining solvent composition in the polymer and ambient liquid. The availability (or lack thereof) of necessary transport and equilibrium data is the greatest obstacle in designing a CFST for solvent removal from spheres.

Acknowledgment

The authors wish to acknowledge Olin Corporation, St. Marks, Florida, for financial support and for generation and analysis of the pilot-plant data.

Notation

C = dimensionless concentration
D = solvent diffusivity
D_{OI} = constant preexponential factor for component I
E = effective diffusion activation energy
$E(\theta)$ = residence time distribution frequency function
f = fraction solvent removed from sphere
Fo_M = mass-transfer Fourier number, $D\tau/R^2$
k = mass-transfer coefficient
M = number of time intervals
N = model parameter describing mixing conditions in system
r = dimensionless length
R = sphere radius
R = gas constant
Sh = Sherwood number, kR/D
T = temperature
V = sphere volume
V_I^* = specific critical hole free volume of component I required for a jump
V_I^0 = specific volume of pure component I at the temperature of interest
w = mass fraction in solid phase
x = mass fraction in liquid phase

Greek letters

β = overlap factor
θ = time
ξ = transfer efficiency
ρ = density
τ = mean residence time
ϕ = fraction of solvent removed from all spheres in system
χ_{Ip} = ratio of critical molar volume of a jumping unit of component I to critical molar volume of jumping unit of polymer, $V_I^* M_{jI}/V_p^* M_{jp}$

Subscripts and Superscripts

1 = first vessel
2 = second vessel
e = exit
h = water
i = ith interval
I = Ith vessel
j = jth vessel
m = mean
n = nth vessel
o = initial
p = polymer
s = solvent
∞ = equilibrium

Literature Cited

Abe, K., K. Yano, S. Kiriyama, K. Nagaoka, Y. Tategami, and T. Shimizu, "Preparation of Microspherical Polyoxyphenylenes with a Narrow Particle Size Distribution," *Chem. Abstr.*, **108**(10), 76137u (1987).

Chiang, J., and R. K. Prudhomme, "Production of monodisperse 5- and 40-μm Polystyrene Spheres," *J. Coll. Interface Sci.*, **122**(1), 283 (1988).

Crank J., *The Mathematics of Diffusion,* Oxford Univ. Press (1956).

Durrans, T. H., *Solvents,* E. H. Davies, ed., 8th ed., Chapman and Hall, London (1971).

Levenspiel, O., *Chem. Reaction Eng.*, Wiley, New York (1972).

Vrentas, J. S., and J. L. Duda, "Diffusion in Polymer–Solvent Systems. I: Reexamination of the Free-volume Theory," *J. Polym. Sci. Polym. Phys. Ed.*, **15**, 403 (1977).

———"Molecular Diffusion in Polymer Solutions," *AIChE J.*, **25**, 1 (1979a).

——— "Diffusion of Large Penetrant Molecules in Amorphous Polymers," *J. Polym. Sci. Polym. Phys. Ed.*, **17**, 1085 (1979b).

Vrentas, J. S., J. L. Duda, and H. C. Ling, "Self-diffusion in Polymer–Solvent–Solvent Systems," *J. Polym. Sci. Polym. Phys. Ed.*, **22**, 459 (1984).

Manuscript received Dec. 27, 1989, and revision received May 10, 1990.